JMEPEG
https://doi.org/10.1007/s11665-024-09291-z

1059-9495/$19.00

ORIGINAL RESEARCH ARTICLE

# Prediction of Flexural Strength with Fuzzy Logic Approach for Fused Deposition Modeling of Polyethylene Terephthalate Glycol Components

*Osman Ulkir and Gazi Akgun*

Submitted: 29 October 2023 / Revised: 3 January 2024 / Accepted: 3 February 2024

**Additive manufacturing (AM) is a preferred industrial manufacturing method for modeling and rapid prototyping of physical systems. The final product in AM must have appropriate mechanical properties, such as flexural strength and be of good quality. The selection of printing parameters is essential for this reason. In this study, three critical printing parameters, such as layer thickness (100-200-300 $\mu$m), raster angle (0-30-60°), and infill density (40-60-80%) were examined. The analysis of variance method was used to look at the relationship between these parameters and the flexure strength of samples fabricated using the fused deposition modeling technique with polyethylene terephthalate glycol material. The experimental design process was performed using Taguchi L9 orthogonal design. Fuzzy logic-based modeling was applied to estimate the flexural strength. The results demonstrated that the infill density is the most important parameter affecting flexural strength compared to the other parameters. The highest strength of 57.76 MPa was achieved when the layer thickness, raster angle, and infill density were set to 100 $\mu$m, 60°, and 80%, respectively. The fuzzy logic provided a high-accuracy estimation of the flexural strength with a maximum percentage error of 2.65%. Consequently, it was determined that the model and experimental results were in agreement.**

**Keywords** additive manufacturing, FDM, flexural strength, fuzzy logic, PETG, Taguchi

## 1. Introduction

Additive manufacturing (AM), or 3D printing is the process of creating a product as the final output from a 3D model prepared digitally. Although there are many AM methods that depend on the type of material used, all methods work according to the same principle (Ref 1, 2). In this principle, the material is created layer-by-layer to obtain the final product. It is possible to create complex shapes using less material in the AM process, unlike in traditional machining (Ref 3). Another important advantage is that it can produce all parts in a single structure (Ref 4). Thus, production costs decrease and efficiency increases in the industrial production process (Ref 5, 6). Such advantages have increased the use of AM technology and have made it preferred in many sectors, such as medicine, automotive, architecture, robotic, and aviation (Ref 7, 8).

There are different fabrication methods in AM technology (Ref 9-12). Among these methods, FDM, a material extrusion-based technology, is widely preferred in the industry. Polymer-based materials are used in the FDM method (Ref 13-18). There is a bias that the mechanical properties of the samples fabricated by this method are not sufficient. 3D printer printing parameters such as fill rate, raster angle, nozzle temperature, table temperature, layer thickness, and printing speed contribute significantly to the mechanical properties, productivity, and quality of the fabricated samples. Consequently, studying the effects of printing factors and predicting results using appropriate process parameters is critical to improve the mechanical properties of printed components (Ref 19, 20). In the current study, three printing parameters (layer thickness, raster angle, and infill density) were determined and the flexural strength properties of the samples fabricated using the FDM technique with PETG material were revealed. The mechanical properties of PETG material against flexure can be determined by examining this feature. However, the determined printing parameters are preferred in many studies, it has been revealed through experimental studies that they affect the flexural strength (Ref 21-23).

There are not enough studies in the literature on improving and predicting flexural strength (Ref 24, 25). Current studies have mostly focused on improving the tensile strength, hardness, and roughness mechanical properties of 3D printed samples (Ref 26-28). Tura and Mamo presented an experimental investigation in terms of flexural strength for the quality analysis of parameters on parts produced by FDM (Ref 29). Taguchi's L18 mixed orthogonal array approach was used to adjust the printing parameters. Layer height, scanning width, scanning angle, and orientation angle were preferred as parameters. A hybrid genetic algorithm and response surface methods, the response surface approach, and the Taguchi method were used to look at and improve how the parameters affected the results of the experiments. Atakok et al. used the

**Osman Ulkir**, Department of Electric and Energy, Mus Alparslan University, Mus, Turkey; and **Gazi Akgun**, Department of Mechatronics Engineering, Marmara University, Istanbul, Turkey. Contact e-mail: o.ulkir@alparslan.edu.tr.



Published online: 29 February 2024

Taguchi method to investigate the effects of FDM manufacturing parameters on the tensile strength, three-point flexural strength, and impact strength of 3D printed PLA and recycled polylactic acid (Re-PLA) (Ref 30). The FDM printing parameters were established as follows: filaments (PLA, Re-PLA), layer thickness (0.15-0.20-0.25 mm), infill rates (30-50-70%), and infill structure (Rectilinear). All performed tests values were found to be directly proportional to infill rates in the study. The optimum results were 0.25 mm, 70%, and PLA for all test results; layer thickness, infill rates, and filament materials, respectively. They were calculated to be 60.006 MPa, 16.961 kJ/m$^2$ at Izod impact strength, 125.423 MPa at three-point bending strength. Zisopol et al. demonstrated the effect of printing parameters on the bending strength of PLA, and ABS printed samples by applying the Taguchi method and ANOVA of 3-point bending test results (Ref 31). Rabinowitz et al. used the Taguchi method to optimize FDM additive manufacturing to maximize the flexural strength of 3D printed polyaryletherketone samples (Ref 32). 3D printed (3DP) carbon fiber-reinforced polyetherketoneketone (CFR PEKK), 3D printed and pressed (3DP + P) CFR PEKK, and injection molded medical grade polyetheretherketone (PEEK) were analyzed as a control. Fracture surfaces were analyzed by scanning electron microscopy (SEM). Parameters changed in the optimization included nozzle diameter, layer height, print speed, raster angle, and nozzle temperature. The results of this study support the hypothesis that subsequent consolidation of 3DP samples improves mechanical properties. Mamo et al. stated that choosing the right printing parameter is important to obtain quality products with suitable properties, such as flexural strength (Ref 33). In this direction, they conducted experimental studies by determining four process variables. ABS material and the FDM method were used in the production of the samples. They developed a fuzzy logic-based prediction model based on input and output parameters. The results revealed that the proposed model and the experimental data were in good agreement. According to the studies, the mechanical properties of the final component fabricated with FDM are highly affected by the printing parameters.

In this study, flexure strength measurements of three-point bending test parts fabricated on an FDM-type 3D printer with layer thickness (100-200-300 $\mu$m), raster angle (0-30-60°), and infill density (40-60-80) printing parameters were examined. PETG material was used in the fabrication of the parts. The experimental design process was performed using the Taguchi method. Flexural samples were fabricated according to the ASTM D790 standard. Taguchi, ANOVA, and contour plots were employed to explore the impact of each performance characteristic. The flexural strength was predicted using fuzzy logic model and compared with the experimental results. Consequently, it was determined that the model and experimental results were in agreement.

## 2. Materials and Methods

### 2.1 Experimental Procedure

A Zaxe Z1 Plus 3D printer was used in the fabrication of the flexural test samples using the fused deposition modeling (FDM) method. Although the fabrication volume of the printer is 300 × 300 × 300 mm, it has a layer resolution of 50-400 microns and a printing speed of 10-300 mm/s. The additive manufacturing can be performed using thermoplastic polymer materials, such as acrylonitrile butadiene styrene (ABS), polylactic acid (PLA), thermoplastic polyurethane (TPU), and polyethylene terephthalate glycol (PETG) with this printer. In this study, PETG, a polymer commonly employed in FDM, was utilized for the fabrication of samples. PETG is characterized by high hardness, durability, impact resistance, and lightweight properties. It is used to produce water bottles, food packaging, and countless other common plastic products. The properties of the PETG material are given in Table 1.

In FDM, a material extrusion additive manufacturing technique, polymers serve as the filament. The filament, heated to a molten state, is extruded through the 3D printer's nozzle. The nozzle's three degrees of freedom (DoF) enable it to deposit the polymer on the build plate based on G-code instructions from standard triangle language (STL) files. The principle of the FDM process is given in a schematic diagram in Figure 1(a). The continuous feeding of the filament through the extruder and nozzle, driven by rollers, results in layer-by-layer deposition on the build plate. The printer nozzle navigates according to spatial coordinates from the original computer-aided design (CAD) model until the desired size and shape are achieved. Extrusion quality depends on the thermoplastic filament properties, leading to printer designs tailored to specific materials.

The ASTM D790 standard was preferred for sizing flexural test samples. The technical drawing and dimensions of the samples are shown in Figure 1(b). The samples prepared according to this standard have dimensions of 125 × 12.7 × 3.2 mm in length, width, and thickness. The 3-point bending test is usually performed on brittle materials rather than a tensile test. Flexural test studies were conducted on a 50-kN force transducer capacity machine (AGS-X, Shimadzu) using the ASTM D790 standard. The mandrel and support diameters were fixed in accordance with the standard in the tests. After the assemblies were fixed, both PETG materials were placed on the supports for the 3-point bending test specimens, and the specimens were bent with the help of a mandrel by applying the load. Experimental studies were performed at a speed of 1 mm/s. Mechanical property data measured during the experiment were recorded using software. Experimental studies were carried out according to eight experiments determined according to the Taguchi method. Maximum flexural strength values in all experiments are given in Table 3. Flexural strength-strain diagrams resulting from the 3-point bending test of some experiments are shown in

**Table 1 Properties of the polyethylene terephthalate glycol filament material**

| Properties | Values |
|---|---|
| Material | PETG |
| Filament color | Yellow |
| Diameter of filament, mm | 1.75 |
| Table temperature, °C | 70-100 |
| Nozzle temperature, °C | 230-260 |
| Tensile strength, MPa | 53 |
| Flexural strength, MPa | 77 |
| Dielectric strength, V/mil | 410 |

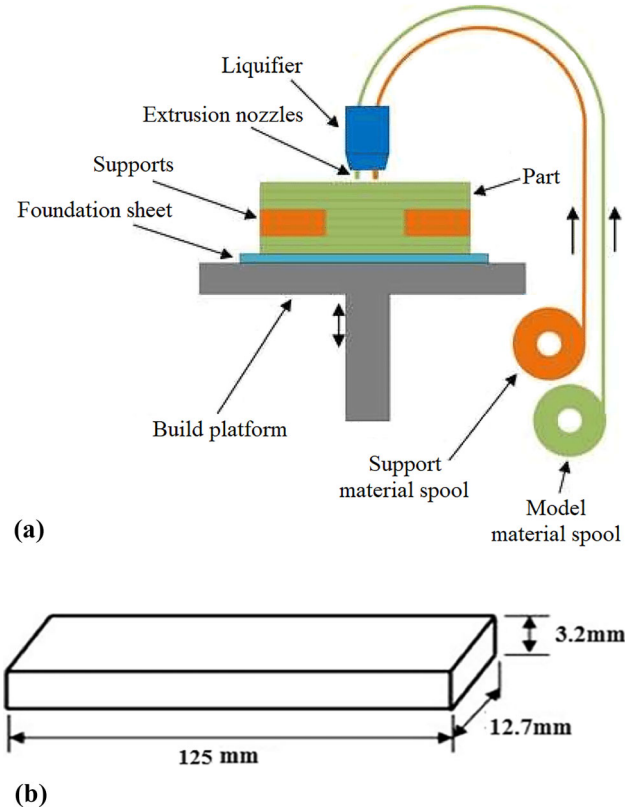


**Fig. 1** (a) Fused deposition modeling printing process (b) Technical drawing of the flexural specimen

Figure 2. Flexural strength values for experiment 3-5-7-8 were measured as 57.76, 46.86, 42.82, and 36.79 MPa, respectively.

### 2.2 Design of the Experiment

In this study, the Taguchi method was used to minimize the number of experiments. Taguchi is the method used to reverse or improve productivity during research and development to obtain a high-quality product at a low cost and in a short time (Ref 34, 35). In the introduction section, it was stated that printing parameters in the AM process have a significant impact on the mechanical properties of the final product components. In the current study, the flexural strength properties of samples fabricated by FDM technique using PETG material were examined. Three different printing parameters were determined for the 3D printer during fabrication. Layer thickness ($\mu$m), raster angle (°), and infill density (%) were selected as printing parameters. It has been revealed in many studies that these parameters have a significant effect on flexural strength. The effectiveness of printing parameters on the flexural strength of PETG samples has been proven by experimental studies. There are three levels for each printing parameter in the designed experimental process. The other printing parameters required for the fabrication process were kept constant in all experimental stages. The printing parameters and their ranges studied are given in Table 2.

The experimental design was made using the Taguchi L9 vertical array. In this design, the signal-to-noise ($S/N$) ratio was used to optimize the determined parameters, ensure stability, and ensure minimum process variability. ANOVA was applied to define and model the relationship between the flexural strength and printing parameters obtained from the measurements. A total of nine experiments were employed based on the Taguchi mixed orthogonal design (Table 3).

### 2.3 Fuzzy Logic Method

A fuzzy logic-based model is proposed to predict the flexure strength values. The fuzzy logic method is frequently used in applications in the field of artificial intelligence (Ref 36, 37). Because this method does not require mathematical modeling, it can be easily applied to complex nonlinear systems. Fuzzy logic principles do not work like classical logic principles. It is not the binary operating system seen in computers. There are no completely right or completely wrong values in fuzzy logic principles. Instead, uncertain options such as false or close to true, partially true, and partially false are also included and graded within the framework of rules (Ref 38, 39).

A fuzzy system defines sets and rules by associating all inputs with all outputs. The working structure of fuzzy systems resembles the workings of a mathematical cause and effect function (Ref 40, 41). One of the most important concepts in fuzzy systems is fuzzy rules. Fuzzy rules include fuzzy control rules designed to achieve the control purpose (Ref 42). The main purpose of this stage is to express expert knowledge in a cause and effect relationship. A fuzzy inference system consists of four stages (Figure 3). These are fuzzification, fuzzy inference system, defuzzification, and knowledge bases. First, all input variables are converted into fuzzification variables in the 'fuzzification' section. Trapezoidal, Gaussian, and triangular membership functions are used for this process. Then, in the 'fuzzy inference system' section, we obtain fuzzy output values for matching inputs by using the knowledge base containing fuzzy IF-THEN rules and membership functions. Finally, in the 'defuzzification' section, the blurry output is converted to a non-fuzzy value and applied to the output.

The first step in modeling with fuzzy logic is to define the input and output parameters. While layer thickness, raster angle, and infill density were determined as the inputs of the system, flexural strength was determined as the output. The inputs and outputs of the fuzzy logic system are shown in Figure 4. The system output is defined as the flexural strength values measured because of the 3-point bending test. Input parameters are defined as the printing parameters that affect the output variable and are the most preferred in the literature. The minimum and maximum values of the input and output parameters were determined with reference to the values in Tables 2 and 3. The proposed fuzzy logic prediction model was implemented using MATLAB software. Mamdani was used as the fuzzy inference system.

The values of membership functions are adjusted according to the upper and lower limits of the inputs and outputs in fuzzy logic modeling. As a result of Taguchi analysis, upper-lower limits and rules for parameter values were determined. Twenty rules were created to define the relationship between these parameters. The fuzzy model was defined as follows; method: min, or method: max, implication: min, aggregation: max, and defuzzification method: centroid. The input and output parameters are represented by linguistic variables or fuzzy membership functions in a Gaussian shape as shown in Figure 5.

In the Gaussian membership function employed for 'Layer Thickness' input, 'Low' for values in the range [100-200 $\mu$m], 'Medium' for values in the range [140-260 $\mu$m], and 'High' for values in the range of [200-300 $\mu$m] were used (Figure 5(a)). In

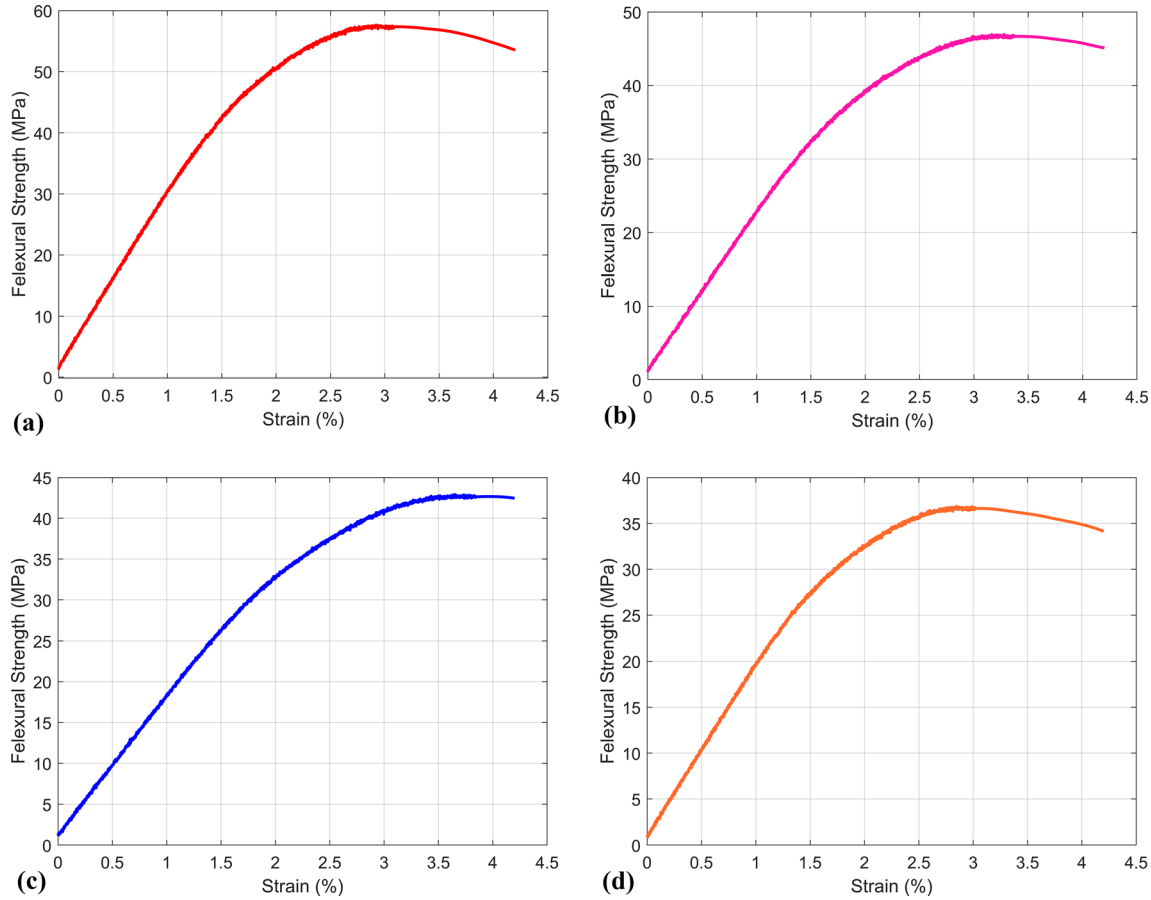


**Fig. 2** Flexural strength-strain diagrams of 3-point bending tests of some experiments (a) experiment 3 (b) experiment 5 (c) experiment 7 (d) experiment 8

**Table 2 Flexural strength factors and levels of the control Taguchi L9**

| | | | Level | | |
|---|---|---|---|---|---|
| **Factors** | **Symbol** | **Units** | **− 1** | **0** | **1** |
| Layer thickness | LT | $\mu$m | 100 | 200 | 300 |
| Raster angle | RA | ° | 0 | 30 | 60 |
| Infill density | ID | % | 40 | 60 | 80 |

the Gaussian membership function employed for 'Raster Angle' input, 'Low' for values in the range [0-30°], 'Medium' for values in the range [10-50°], and 'High' for values in the range of [30-60°] were used (Figure 5(b)). In the Gaussian membership function employed for 'Infill Density' input, 'Low' for values in the range [40-60%], 'Medium' for values in the range [45-75%], and 'High' for values in the range of [60-80%] were used (Figure 5(c)). In the Gaussian membership function employed for 'Flexural Strength' output, 'Extremely Low' for values in the range [36-40 MPa], 'Very Low' for values in the range [36-44 MPa], 'Low' for values in the range [40-48 MPa],

**Table 3 L9 orthogonal array Taguchi flexural test results and signal/noise ratios**

| Run | Layer thickness, $\mu$m | Raster angle, ° | Infill density, % | Flexural strength, MPa | Signal/noise, dB |
|---|---|---|---|---|---|
| 1 | 100 | 0 | 40 | 39.63 | 31.7385 |
| 2 | 100 | 30 | 60 | 45.54 | 33.3565 |
| 3 | 100 | 60 | 80 | 57.76 | 35.0808 |
| 4 | 200 | 0 | 60 | 39.89 | 31.7968 |
| 5 | 200 | 30 | 80 | 46.86 | 33.4160 |
| 6 | 200 | 60 | 40 | 39.75 | 31.9867 |
| 7 | 300 | 0 | 80 | 42.82 | 32.4277 |
| 8 | 300 | 30 | 40 | 36.79 | 31.0752 |
| 9 | 300 | 60 | 60 | 43.58 | 32.5841 |

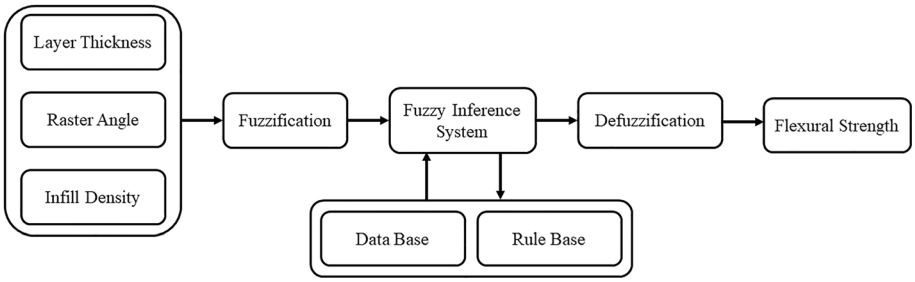


**Fig. 3** The basic structure of the fuzzy logic controller with inputs and output

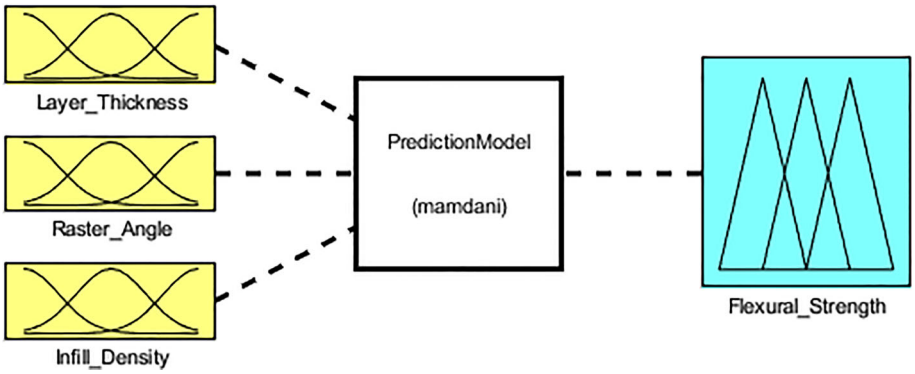


**Fig. 4** Schematic diagram of the fuzzy logic system with three inputs and one output response

'Normal' for values in the range [43-51 MPa], 'High' for values in the range [47-54 MPa], 'Very High' for values in the range [50-58 MPa], and 'Extremely High' for values in the range of [54-58 MPa] were used (Figure 5(d)).

## 3. Results and Discussion

### 3.1 Evaluation of the Process Parameters

Taguchi design is a set of methodologies in which the inherent variability of materials and manufacturing processes is considered during the design phase. In this design, the signal-to-noise ($S/N$) ratio is used to achieve a robust system and make the process indifferent to noise factors. Thus, an optimum-quality design is created with minimal changes. This study aimed to optimize and predict the flexural strength properties of PETG samples fabricated using layer thickness, raster angle, and infill density parameters. Thus, 'the larger is better' property was used during the analysis with Taguchi method.

The Taguchi experimental design results in Table 3 were evaluated by applying analysis of variance (ANOVA) to identify important printing parameters affecting performance measurements. The ANOVA results are given in Table 4. The confidence interval was determined to be 95% during the analysis. According to the results, the most important parameter affecting flexural strength is the infill density. This parameter was followed by layer thickness and raster angle in order of importance. The $F$ and $P$ tests were used to verify the significance of the results in the ANOVA. According to these tests, the higher the $F$ value and the lower the $P$ value, the greater the effect of the process parameters on performance. A $P$ value of less than 0.05 makes the parameters significant. The $P$ value of all parameters is less than 0.05 in the table. This proves that the selected printing parameters have a significant effect on flexural strength. The contribution rates of the printing parameters to the flexural strength were also calculated as percentages (Table 4). However, the infill density has the highest effect on strength (48.42%), the contribution rates of layer thickness and raster angle were calculated at 28.51 and 21.73%, respectively.

Main effect analysis was performed to calculate the optimum printing parameters. Figure 6 shows the main effect plot for the effects and levels of the three-point bending strength parameters. This graph shows the change in the flexural strength value with printing parameters. It can be seen from the main effect graph that the infill density parameter has a significant effect on flexural strength. The effect rates of the other parameters were close to each other. An increase in infill density and raster angle values has increased the flexural strength. However, an increase in layer thickness parameter has decreased the strength value. The relationship between the raster angle, and infill density parameters, and three-point bending strength is proportional. Among the preferred printing parameters, the best values are layer thickness of 100 $\mu$m, raster angle of 60°, and infill density of 80%.

Figure 7 shows the contour plot graphs that show the relationship between PETG component flexural strength and printing variables. Infill density is an important factor that influences the flexural strength properties. As clearly shown in Figure 7(b) and (c), increasing infill density has a significant impact on flexural strength. Raster angle is another significant factor that could influence flexural strength. As can be clearly seen in Figure 7(a) and (b), 60° of raster angle gives the highest flexural strength. The effect of layer thickness on flexural strength is shown in Figure 7(a) and (c). It can be seen that when the layer thickness increases, the flexural strength value tends to decrease. As a result, the flexural strength values were

high at points where the infill density and raster angle parameters were high and the layer thickness parameter was low (Figure 7).

### 3.2 Evaluation of Fuzzy Logic Results

Modeling software was used on the basis of the information given in Table 3 to find the results of the proposed fuzzy logic prediction. 3D surface plots were created to see the relationship between input and output parameters. Fuzzy logic result graphs of the flexural strength with printing parameters are given in Figure 8. It can be clearly seen that the input parameters have a significant effect on flexural strength. The effect of the infill density parameter is quite high from the results. This parameter is followed by layer thickness and raster angle. The highest flexural strength values were found in regions where infill density and raster angle were high (Figure 8(a), (b) and (c)). The highest flexure strength value was measured in the parameters in Figure 8(b).

The results obtained with the fuzzy logic method overlapped with the contour graphs of flexural strength in Figure 7. Although different methodologies were applied, similar results were obtained. In both methods, the most important parameter affecting flexural strength values was infill density. The effect of other parameters gave similar results. Strength values were also close to each other.

After the fuzzy logic modeling process, the defuzzification process is performed to give the output parameter a number. After this process, a comparison is made between the prediction model outputs and the experimental results. The output data of the experimental data, fuzzy model, and Taguchi model are presented graphically in Figure 9. The proposed fuzzy logic model predicted the flexural strength data more successfully than the Taguchi method. In the fuzzy model, the maximum error amount was 2.65% in sample 4, while this value was calculated as 4.58% for Taguchi. The results obtained revealed that the proposed fuzzy model is a very effective method for determining parameter properties.

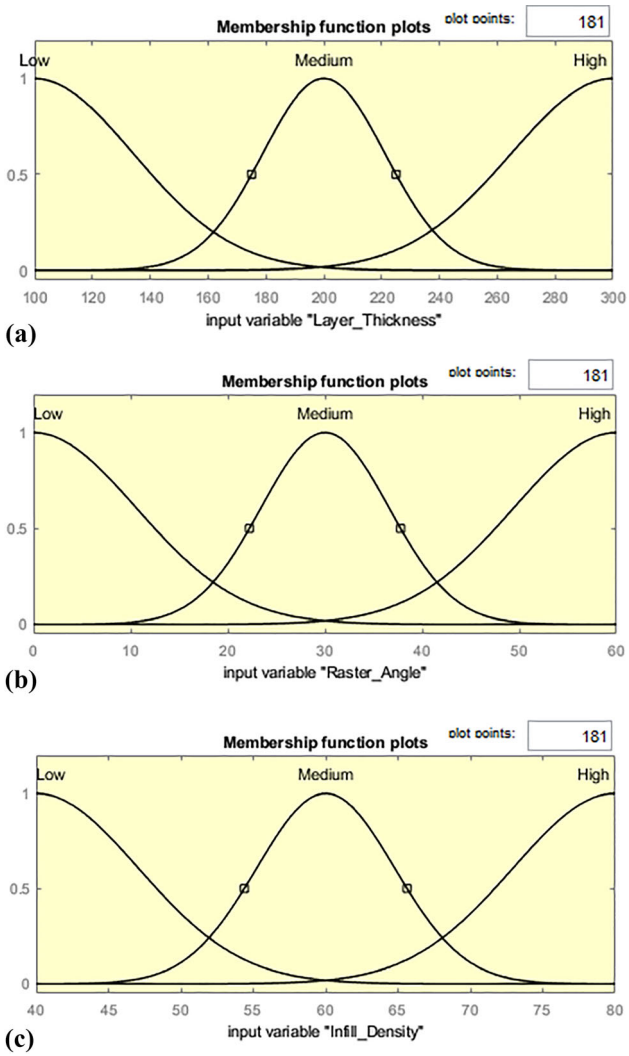


**Fig. 5** Gaussian membership functions of printing parameters (a) layer thickness (b) raster angle (c) infill density (d) flexural strength

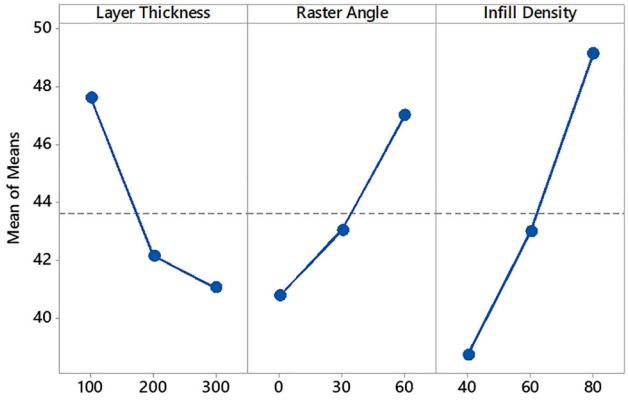


**Fig. 6** Main effects plot for means of FDM process parameters

**Table 4 The analysis of variance for flexural strength**

| Factors | Degree of freedom (DF) | Sum of squares (s) | Mean Square (MS) | *F*-Value | *P*-Value | Contribution, % |
|---|---|---|---|---|---|---|
| Layer thickness | 2 | 85.641 | 42.820 | 34.34 | 0.028 | 28.51 |
| Raster angle | 2 | 65.011 | 32.505 | 26.07 | 0.037 | 21.73 |
| Infill density | 2 | 163.685 | 81.842 | 65.63 | 0.015 | 48.42 |
| Error | 2 | 2.494 | 1.247 | ... | ... | 1.34 |
| Total | 8 | 316.830 | … | ... | ... | 100 |

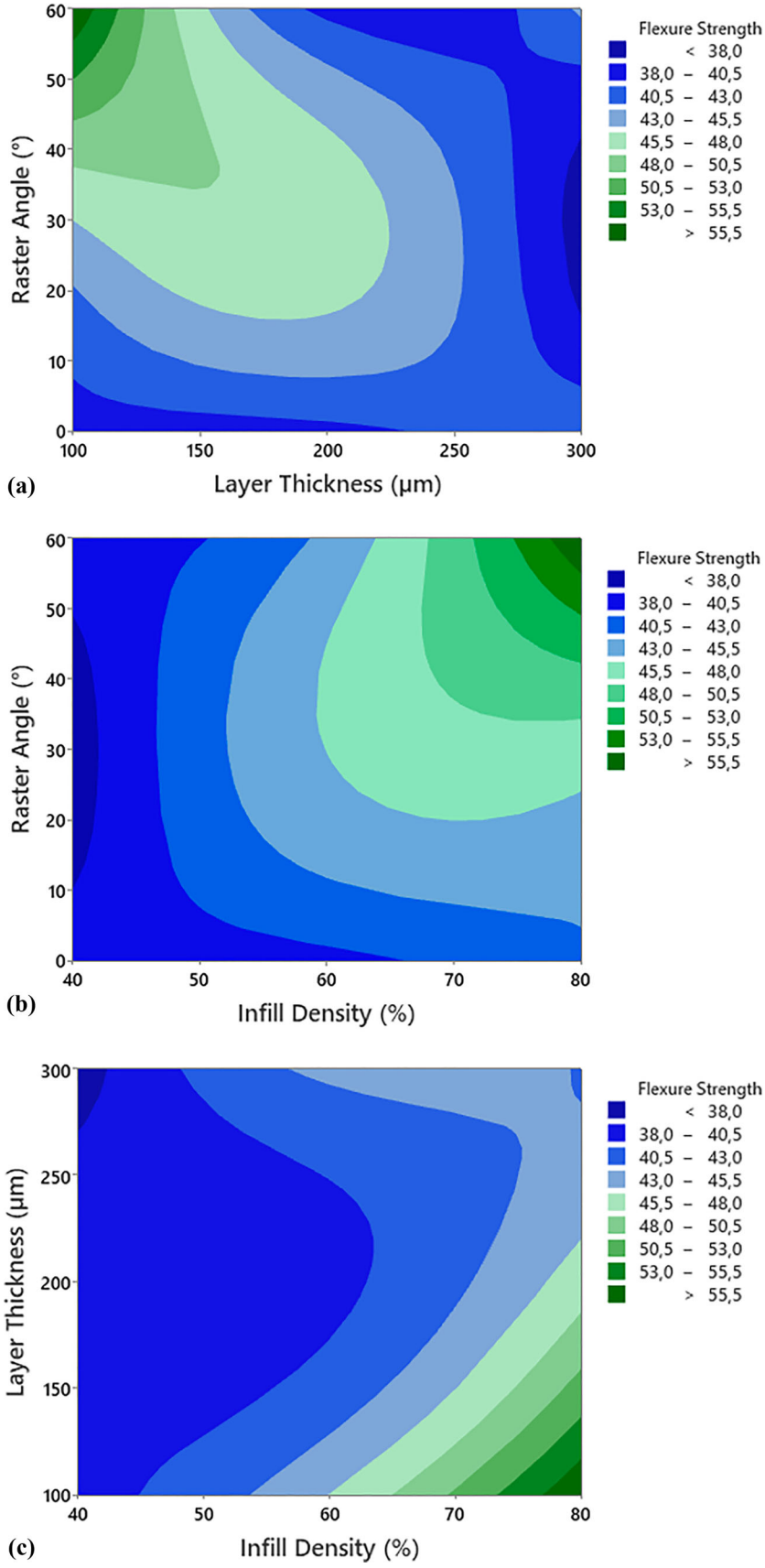


**Fig. 7** Contour plots of flexural strength with printing parameters (a) layer thickness vs. raster angle (b) infill density vs. raster angle (c) infill density vs. layer thickness

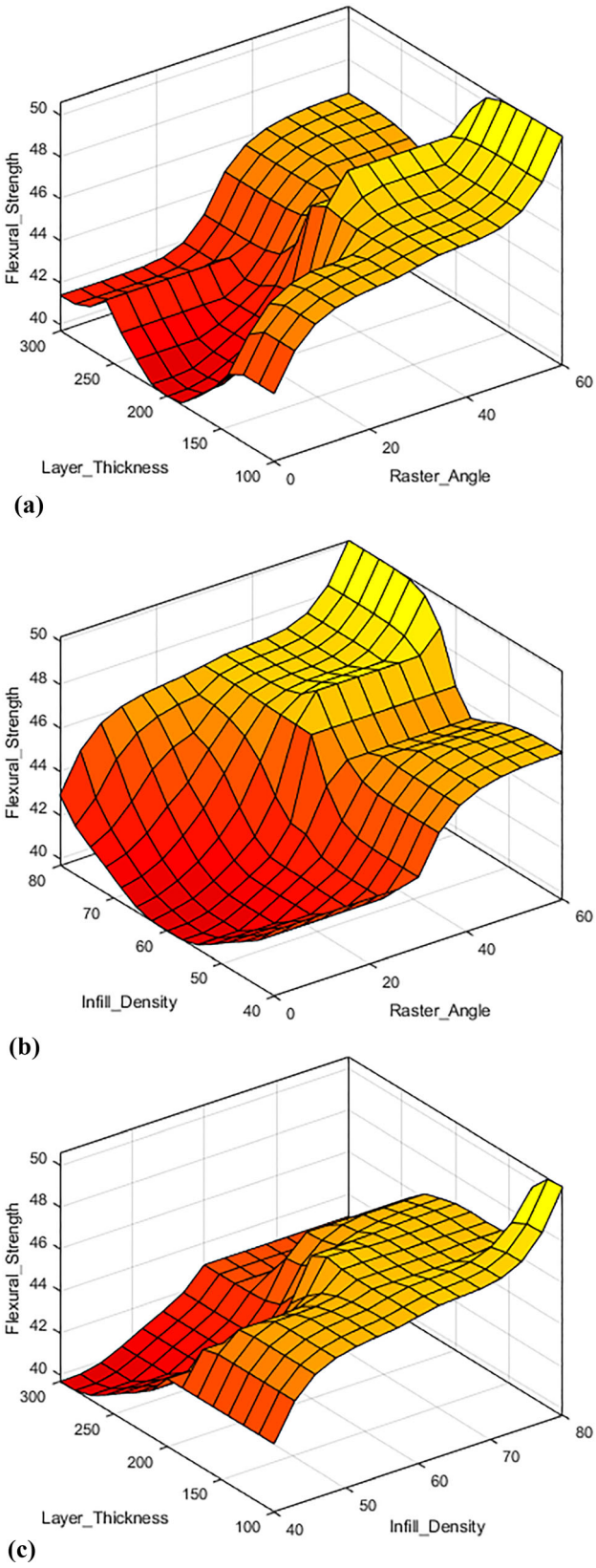


**Fig. 8** Fuzzy logic result plots of flexural strength with printing parameters (a) layer thickness vs. raster angle (b) infill density vs. raster angle (c) infill density vs. layer thickness

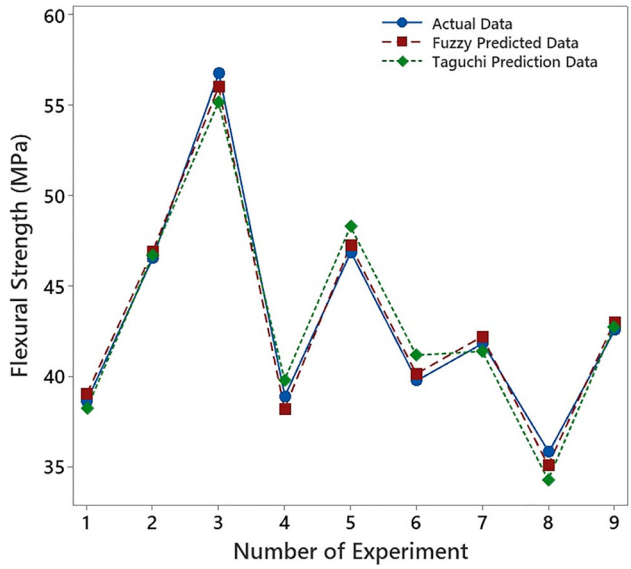


**Fig. 9** Comparison of the actual and predicted output

## 4. Conclusions

This research proposed a fuzzy logic model to predict the flexural strength for layer thickness, raster angle, and infill density on PETG samples fabricated using the fused deposition modeling (FDM) method. The flexural strength properties of PETG materials were examined for the first time with a fuzzy logic model in this study. The experimental design process was performed according to the L9 orthogonal Taguchi method. The relationship between compression parameters and flexural strength was revealed using ANOVA and main effect graphs. Because of the analyses, it was determined that the most important parameter affecting flexural strength is the infill density. The contribution rate of this parameter was 48.42%. The contribution rates of layer thickness and raster angle were calculated as 28.51 and 21.73%, respectively. The highest strength was obtained when the layer thickness, raster angle, and infill density were set to 100 $\mu$m, 60°, and 80%, respectively (experiment 3). The flexural strength value in this experiment was 57.76 MPa. Taguchi experimental data were used to develop the proposed fuzzy logic model. The success of the prediction models was compared in terms of percentage error. The fuzzy logic provided a high-accuracy estimation of the flexural strength with a maximum percentage error of 2.65%. As a result, it was determined that the model and experimental results were in agreement. It has been demonstrated through experimental studies that the flexural strength of parts fabricated by FDM can be predicted with fuzzy logic. The results can be used as a reference for other studies. Our next research will focus on optimizing flexural strength through the application of machine learning methodologies, including artificial neural networks, k-nearest neighbor's algorithm, genetic algorithm, and support vector machines.

## Funding

The author received no financial support for the research, authorship, and/or publication of this article.

## Data and Code Availability

All data underlying the results are available as part of the article, and no additional source data are required.

## Conflict of interest

The author declares no conflict of interest.

## Ethical Approval

The author declares that this study does not require ethical approval.

## References

1. N. Li, S. Huang, G. Zhang, R. Qin, W. Liu, H. Xiong, G. Shi, and J. Blackburn, Progress in Additive Manufacturing on New Materials: A Review, *J. Mater. Sci. Technol.*, 2019, **35**(2), p 242–269.
2. H. Kim, Y. Lin, and T.-L.B. Tseng, A Review on Quality Control in Additive Manufacturing, *Rapid Prototyp. J.*, 2018, **24**(3), p 645–669.
3. Y. Zhang, L. Wu, X. Guo, S. Kane, Y. Deng, Y.-G. Jung, J.-H. Lee, and J. Zhang, Additive Manufacturing of Metallic Materials: A Review, *J. Mater. Eng. Perform.*, 2018, **27**(1), p 1–13.
4. M.S. Bayraklilar, Dimensional Accuracy of Acrylonitrile Butadiene Styrene Material Produced by Additive Manufacturing Method, *J. Mater. Eng. Perform.*, 2023 https://doi.org/10.1007/s11665-023-08205-9
5. Y. Qin, Q. Qi, P.J. Scott, and X. Jiang, Status, Comparison, and Future of the Representations of Additive Manufacturing Data, *Comput. Des.*, 2019, **111**, p 44–64.
6. B. Ezair, S. Fuhrmann, and G. Elber, Volumetric Covering Print-Paths for Additive Manufacturing of 3D Models, *Comput. Des.*, 2018, **100**, p 1–13.
7. M. Javaid and A. Haleem, Additive Manufacturing Applications in Medical Cases: A Literature Based Review, *Alexandria J. Med.*, 2018, **54**(4), p 411–422.
8. T. Pereira, J.V. Kennedy, and J. Potgieter, A Comparison of Traditional Manufacturing vs Additive Manufacturing, the Best Method for the Job, *Procedia Manuf.*, 2019, **30**, p 11–18.
9. M. Carlotti and V. Mattoli, Functional Materials for Two-Photon Polymerization in Microfabrication, *Small*, 2019, **15**(40), p 1902687.
10. J. Huang, Q. Qin, and J. Wang, A Review of Stereolithography: Processes and Systems, *Processes*, 2020, **8**(9), p 1138.
11. S.A.M. Tofail, E.P. Koumoulos, A. Bandyopadhyay, S. Bose, L. O'Donoghue, and C. Charitidis, Additive Manufacturing: Scientific and Technological Challenges, Market Uptake and Opportunities, *Mater. Today*, 2018, **21**(1), p 22–37.
12. H. Li, J. Dai, Z. Wang, H. Zheng, W. Li, M. Wang, and F. Cheng, Digital Light Processing (DLP)-based (Bio) Printing Strategies for Tissue Modeling and Regeneration, *Aggregate*, 2023, **4**(2), p e270.
13. Q. Ding, X. Li, D. Zhang, G. Zhao, and Z. Sun, Anisotropy of Poly(Lactic Acid)/Carbon Fiber Composites Prepared by Fused Deposition Modeling, *J. Appl. Polym. Sci.*, 2020, **137**(23), p 48786.
14. T.N.A.T. Rahim, A.M. Abdullah, and H. Md Akil, Recent Developments in Fused Deposition Modeling-Based 3D Printing of Polymers and Their Composites, *Polym. Rev.*, 2019, **59**(4), p 589–624.
15. P. Awasthi and S.S. Banerjee, Fused Deposition Modeling of Thermoplastic Elastomeric Materials: Challenges and Opportunities, *Addit. Manuf.*, 2021, **46**, p 102177.
16. M. Nabipour, B. Akhoundi, and A. Bagheri Saed, Manufacturing of Polymer/Metal Composites by Fused Deposition Modeling Process with Polyethylene, *J. Appl. Polym. Sci.*, 2020, **137**(21), p 48717.
17. T. Kuipers, E.L. Doubrovski, J. Wu, and C.C.L. Wang, A Framework for Adaptive Width Control of Dense Contour-Parallel Toolpaths in Fused Deposition Modeling, *Comput. Des.*, 2020, **128**, p 102907.
18. A. Alafaghani and A. Qattawi, Investigating the Effect of Fused Deposition Modeling Processing Parameters Using Taguchi Design of Experiment Method, *J. Manuf. Process.*, 2018, **36**, p 164–174.
19. M. Heidari-Rarani, N. Ezati, P. Sadeghi, and M. Badrossamay, Optimization of FDM Process Parameters for Tensile Properties of Polylactic Acid Specimens Using Taguchi Design of Experiment Method, *J. Thermoplast. Compos. Mater.*, 2022, **35**(12), p 2435–2452.
20. D. Syrlybayev, B. Zharylkassyn, A. Seisekulova, M. Akhmetov, A. Perveen, and D. Talamona, Optimisation of Strength Properties of FDM Printed Parts—A Critical Review, *Polymers (Basel)*, 2021, **13**(10), p 1587.
21. J. Brackett, D. Cauthen, J. Condon, T. Smith, N. Gallego, V. Kunc, and C. Duty, The Impact of Infill Percentage and Layer Height in Small-Scale Material Extrusion on Porosity and Tensile Properties, *Addit. Manuf.*, 2022, **58**, p 103063.
22. S.S. Iyer and O. Keles, Effect of Raster Angle on Mechanical Properties of 3D Printed Short Carbon Fiber Reinforced Acrylonitrile Butadiene Styrene, *Compos. Commun.*, 2022, **32**, p 101163.
23. O. Ulkir and G. Akgun, Predicting and Optimising the Surface Roughness of Additive Manufactured Parts Using an Artificial Neural Network Model and Genetic Algorithm, *Sci. Technol. Weld. Join.*, 2023, **28**(7), p 548–557.
24. N. Nawafleh and E. Celik, Additive Manufacturing of Short Fiber Reinforced Thermoset Composites with Unprecedented Mechanical Performance, *Addit. Manuf.*, 2020, **33**, p 10110.
25. J.S. Chohan, N. Mittal, R. Kumar, S. Singh, S. Sharma, J. Singh, K.V. Rao, M. Mia, D.Y. Pimenov, and S.P. Dwivedi, Mechanical Strength Enhancement of 3D Printed Acrylonitrile Butadiene Styrene Polymer Components Using Neural Network Optimization Algorithm, *Polymers (Basel)*, 2020, **12**(10), p 2250.
26. N. Jayanth, P. Senthil, and C. Prakash, Effect of Chemical Treatment on Tensile Strength and Surface Roughness of 3D-Printed ABS Using the FDM Process, *Virtual Phys. Prototyp.*, 2018, **13**(3), p 155–163.
27. N. Kladovasilakis, P. Charalampous, K. Tsongas, I. Kostavelis, D. Tzovaras, and D. Tzetzis, Influence of Selective Laser Melting Additive Manufacturing Parameters in Inconel 718 Superalloy, *Materials (Basel)*, 2022, **15**(4), p 1362.
28. D.A. Snelling, C.B. Williams, and A.P. Druschitz, Mechanical and Material Properties of Castings Produced via 3D Printed Molds, *Addit. Manuf.*, 2019, **27**, p 199–207.
29. A.D. Tura and H.B. Mamo, Characterization and Parametric Optimization of Additive Manufacturing Process for Enhancing Mechanical Properties, *Heliyon*, 2022, **8**(7), p e09832.
30. G. Atakok, M. Kam, and H.B. Koc, Tensile, Three-Point Bending and Impact Strength of 3D Printed Parts Using PLA and Recycled PLA Filaments: A Statistical Investigation, *J. Mater. Res. Technol.*, 2022, **18**, p 1542–1554.
31. D.G. Zisopol, I. Nae, A.I. Portoaca, and I. Ramadan, A Statistical Approach of the Flexural Strength of PLA and ABS 3D Printed Parts, *Eng. Technol. Appl. Sci. Res.*, 2022, **12**(2), p 8248–8252.
32. A. Rabinowitz, P.M. DeSantis, C. Basgul, H. Spece, and S.M. Kurtz, Taguchi Optimization of 3D Printed Short Carbon Fiber Polyetherketoneketone (CFR PEKK), *J. Mech. Behav. Biomed. Mater.*, 2023, **145**, p 105981.
33. H.B. Mamo, A.D. Tura, A. Johnson Santhosh, N. Ashok, and D. Kamalakara Rao, Modeling and Analysis of Flexural Strength with Fuzzy Logic Technique for a Fused Deposition Modeling ABS Components, *Mater. Today Proc.*, 2022, **57**, p 768–774.
34. B. Vaissier, J.-P. Pernot, L. Chougrani, and P. Véron, Genetic-Algorithm Based Framework for Lattice Support Structure Optimization in Additive Manufacturing, *Comput. Des.*, 2019, **110**, p 11–23.
35. H. Gholizadeh, M. Goh, H. Fazlollahtabar, and Z. Mamashli, Modelling Uncertainty in Sustainable-Green Integrated Reverse Logistics Network Using Metaheuristics Optimization, *Comput. Ind. Eng.*, 2022, **163**, p 107828.
36. B.M. Moreno-Cabezali, and J.M. Fernandez-Crehuet, Application of a Fuzzy-Logic Based Model for Risk Assessment in Additive Manufacturing R&D Projects, *Comput. Ind. Eng.*, 2020, **145**, p 106529.
37. A. Heidarzadeh, Ö.M. Testik, G. Güleryüz, and R.V. Barenji, Development of a Fuzzy Logic Based Model to Elucidate the Effect of FSW Parameters on the Ultimate Tensile Strength and Elongation of Pure Copper Joints, *J. Manuf. Process.*, 2020, **53**, p 250–259.
38. N. Bagherian-Marandi, M. Ravanshadnia, and M.-R. Akbarzadeh-T, Two-Layered Fuzzy Logic-Based Model for Predicting Court Deci-

sions in Construction Contract Disputes, *Artif. Intell. Law*, 2021, **29**(4), p 453–484.
39. N. Singh, D. Virmani, and X.-Z. Gao, A Fuzzy Logic-Based Method to Avert Intrusions in Wireless Sensor Networks using WSN-DS Dataset, *Int. J. Comput. Intell. Appl.*, 2020, **19**(03), p 2050018.
40. H. Huang, H. Xu, F. Chen, C. Zhang, and A. Mohammadzadeh, An Applied Type-3 Fuzzy Logic System: Practical Matlab Simulink and M-Files for Robotic, Control, and Modeling Applications, *Symmetry (Basel)*, 2023, **15**(2), p 475.
41. K. Kaplan, M. Kuncan, and H.M. Ertunc, (2015) "Prediction of Bearing Fault Size by Using Model of Adaptive Neuro-Fuzzy Inference System," in *2015 23nd Signal Processing and Communications Applications Conference (SIU)*, IEEE, p 1925–1928
42. S. Hrehová, J. Husár, and L. Knapčíková, The Fuzzy Logic Predictive Model for Remote Increasing Energy Efficiency, *Mob. Netw. Appl.*, 2022 https://doi.org/10.1007/s11036-022-02050-1